

# **Partial Hessian vibrational analysis: vapour pressure isotope effects and their relation with non-covalent interactions**

Luis Vasquez\*

*Institute of Applied Radiation Chemistry, Lodz University of Technology, Żeromskiego 116,  
Łódź 90-914, Poland*

E-mail: [luis.vasquez@edu.p.lodz.pl](mailto:luis.vasquez@edu.p.lodz.pl)

February 28, 2022

### Abstract

Stable isotope analysis is regularly used in order to acquire detailed information of physical and chemical processes that a system is undergoing. Experimental data is thus complemented with computational studies, in order to develop theoretical models that can satisfactorily explain and predict a determined phenomenon in similar systems. However, proper estimation of isotope effects remains a challenging task. High levels of theory are demanded in order to correctly describe non-covalent interactions, while large molecular systems are required to mimic solvent effects. Given specifications typically restrict the available theoretical approach to a few electronic structure methods.

In this study equilibrium isotope effects (EIEs) on evaporation to several organic solvents (bromobenzene, dibromomethane, ethanol, methanol, and trichloromethane) in the pure phase are estimated employing Kohn-Sham Density functional theory (KS-DFT) along with full Hessian vibrational analysis (FHVA) and partial Hessian vibrational analysis (PHVA). Both FHVA and PHVA qualitatively predict compounds EIEs. Weakly interacting systems (bromobenzene, dibromomethane, and trichloromethane) display identical EIE values for both, FHVA and PHVA. Whereas for strongly interacting systems (ethanol and methanol), PHVA estimates slightly smaller EIE compared to FHVA. By employing the symmetry-adapted perturbation theory (SAPT) along with independent gradient model (IGM), it was possible to establish how minimal changes in compounds interaction energy affected carbon and bromine EIEs estimation in dibromomethane. Moreover, SAPT and IGM revealed how in ethanol, apparently insignificant intermolecular interactions possessed an enormous impact in carbon position specific isotope effects, which highlight the importance of solvent effects for strongly interacting compounds. The presented results have important implications for correctly comprehending and characterising the role of non-covalent interactions in the prediction of isotope effects, as well as providing a robust test to PHVA for the prediction of EIEs.

# Introduction

Equilibrium isotope effects (EIEs) are one of the most successful tools in biochemistry, geochemistry, and chemistry for meticulously studying exchange reactions during processes such as volatilisation, sorption, and evaporation.<sup>1-4</sup> Given processes are vital to comprehend pollution, biodegradation pathways and remediation of contaminated aquiferous systems like oceans, lakes, and underground reservoirs. Halogenated compounds such as trichloromethane and bromobenzene represent a global concern, given that are not merely perilous pollutants with suspected carcinogen properties, but equally are known for their slow dissolution (per years) in anoxic environments.<sup>4</sup>

Technological advances during the last two decades permit now the accurate measuring of position specific isotope effects, hence providing an valuable insight into the nature of bulk isotope effects. However, precise interpretation of experimental results remains a complex task, predominantly owing to physicochemical phenomena that might be easily overlooked such as diffusion or adsorption, but posses a substantial influence over the outcome.<sup>5,6</sup> For instance, it is conceivable that the diffusion effect vanishes from compounds boiling point on, leaving as result mere EIE or so-called vapour pressure isotope effects (VPIE).<sup>2,7</sup> However when direct measurements are performed at standard conditions, to some extend the diffusion effects are present, under those circumstances the term volatilisation isotope effect (VIEs) is employed to emphasise the temperature factor.

Usually, owing to the quantum nature of EIEs,<sup>8</sup> experimental data is adequately depicted *via* electronic structure calculations. Thus, finding stationary points on a potential-energy surface (PES), the theory of molecular vibrations of molecular systems<sup>9</sup> is employed by the Bigeleisen-Mayer approach for the practical calculation of isotope effects.<sup>8</sup> Predominantly, electron structure calculations based on Kohn-Sham density functional theory (KS DFT)<sup>10</sup> are used. Given choice is motivated mainly by the relative robust performance of density functionals and their affordable computational cost for the full quantum-mechanical treatment of large systems (molecular systems with more than 40 atoms). In practice, the

B3LYP functional<sup>11-14</sup> is likely the most used functional for isotope effects calculation,<sup>9</sup> and although in recent KS DFT benchmarks it does not perform well,<sup>15</sup> its notable ability to predict correctly the isotopic frequency shifts converts it in one of the DFT functionals for excellence. Another exceptional functional is MPW1PW91,<sup>16-18</sup> which has permitted the accurate predictions of hydrogen and carbon VPIEs for fluoroform.<sup>19,20</sup>

Important, and a point often overlooked, is the quality of stationary point atomic positions. It must be remembered that the Hessian is the second derivative of the molecular energy with respect to nuclear coordinates (Cartesian coordinates), therefore undergoing an accurate reproduction of them intentionally serves as a pivotal step in order to calculate reliable isotope effects for the precise reason. Moreover, correctly reproducing compounds interatomic interactions conjointly guarantee solvent effects emulation. Goerigk *et al.* have demonstrated in a recent study that weighted total mean absolute deviation for non-covalent interaction calculated by B3LYP and MPW1PW91 functionals are notably large, especially if dispersion corrections are not included.<sup>15</sup> Therefore, meticulous care during the functional selection is required, given that generally accurate atomic positions implies expensive numerical calculations within the "Jacobs ladder" rungs.

After carefully choosing an adequate DFT functional for the purpose of calculating EIEs, the Hessian matrix must be computed, however, because the Hessian matrix is routinely calculated numerically (finite difference of analytic gradients)<sup>21,22</sup> within KS DFT, even for relatively compact systems its calculation is computationally expensive.<sup>23</sup> In order to surmount given drawback, either software package parallelisation along with more efficient algorithms or rigorous Hessian approximations are been continuously developed.<sup>23-27</sup> The later is appealing, particularly the partial Hessian approach,<sup>28,29</sup> which principle lies on the diagonalisation of a sub-block of the mass-weighted energy second derivative matrix computed for a subgroup of atoms. This pragmatic approach has been successfully employed for characterisation of the infrared spectrum of large transition metals,<sup>30</sup> vibrational analysis of relevant cluster compounds,<sup>31</sup> fingerprint vibrations of adsorbates on surfaces,<sup>28,29,31</sup> and

molecular vibrational energy and entropy.<sup>32</sup> Although partial Hessian<sup>28</sup> or adapted versions have been efficiently implemented in the past for estimation of EIEs,<sup>33,34</sup> those studies did not explore at least one of the following issues i.) the quality of intermolecular interactions compared to experimental data or reliable levels of theory, ii.) equivalent configurations of PES by nuclear coordinates, iii.) effect of partial Hessian in the reduced partition function ratio (RPFR) terms,<sup>8</sup> or iv.) practical limitation of partial Hessian approach.

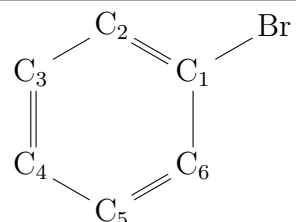
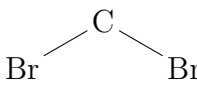
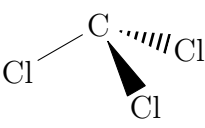
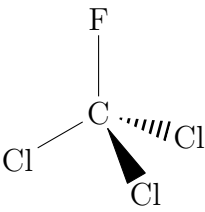
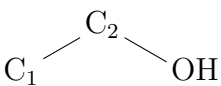
We report on numerical calculation results of EIEs for two organic solvents which mainly interact *via* hydrogen bonds: ethanol, and methanol, and other four highly polluting halogenated compounds bromobenzene, trichlorofluoromethane, dibromomethane, and trichloromethane. EIEs results from full Hessian and partial Hessian vibrational analysis are properly compared, as well as their direct effects on the components of the reduced partition function ratio. Moreover, unique insight into intermolecular interactions of certain studied compounds and their relationship with EIEs are carefully analysed and described.

## Methods

Molecular dynamic simulations were performed for bromobenzene (BB - C<sub>6</sub>H<sub>5</sub>Br), trichlorofluoromethane (CFC - CFCl<sub>3</sub>), dibromomethane (DBM - CH<sub>2</sub>Br<sub>2</sub>), ethanol (ETH - C<sub>2</sub>H<sub>5</sub>OH), methanol (MeOH - CH<sub>3</sub>OH), and trichloromethane (TCM - CHCl<sub>3</sub>) (table 1) using the open-source software LAMMPS (large-scale atomic/molecular massively parallel simulator).<sup>35</sup> Optimized potentials for liquid simulations (OPLS) force field parameters<sup>36,37</sup> from the LigParGen web server<sup>38</sup> have been used for model simulations. Periodic boundary conditions for a cubic box comprising 90 molecules have been properly minimised and brought to equilibrium at standard conditions.

Consequently, for each compound, five clusters containing four molecules were extracted from trajectories of equilibrated MD simulations. Nuclear coordinates of clusters were further optimised using a long-range-corrected (LRC) hybrid functional with non local correlation,

Table 1: Systems used in this study.

Name	Structure
Bromobenzene (BB)	
Dibromomethane (DBM)	
Chloroform (TCM)	
Trichlorofluoromethane (CFC)	
Ethanol (EtOH)	
Methanol (MeOH)	

$\omega$ B97X-V.<sup>39</sup> Basis set double, and triple Dunning’s augmented correlation consistent<sup>40,41</sup> were used. All geometrical optimisations were carefully performed using the SG-2<sup>42</sup> integration grid. Stationary points on the potential surface were confirmed from full Hessian vibrational analysis (FHVA) without imaginary frequencies. During the vibrational analysis the SG-3 grid<sup>42</sup> was employed. All quantum mechanical calculations were carried out in Q-Chem software packages (version 4.4),<sup>43</sup> and were typically restricted to an allowable maximum of 4032 computational hours.

Partial Hessian vibrational analyses<sup>28,31</sup> (PHVA) were performed to clusters for which FHVA was carried out successfull. In PHVA only one molecule was ”active”, *i.e.* the second partial derivatives of the potential with respect to displacement of the atoms is calculated, whereas the other three remained ”frozen”. Given approach was used with each one of the molecules within a cluster.

With the purpose to robustly assess the accuracy of PHVA with respect to FHVA, equilibrium isotope effects (EIE) were properly calculated implementing the Bigeleisen-Mayer approximation from the ratio of the free energies of the isotopologues,<sup>8</sup> thus, using vibrational analysis for Bigeleisen-Mayer approximation gives

$$\frac{s_h}{s_l} f = \prod_i \frac{\nu_{hi}}{\nu_{li}} \frac{\exp(-hc\nu_{li}/2k_B T) / 1 - \exp(-hc\nu_{li}/k_B T)}{\exp(-hc\nu_{hi}/2k_B T) / 1 - \exp(-hc\nu_{hi}/k_B T)} = EIE \quad (1)$$

where  $h$  is the Planck’s constant,  $c$  represents the speed of light in vacuum,  $k_B$  introduces the Boltzmann constant,  $T$  refers to temperature,  $\nu$  indicates the harmonic frequency, and  $(s_h/s_l) f$  is the reduced partition function ratio.

It is worth to note that EIE can be expressed in terms of enrichment factor  $\varepsilon$  as

$$\varepsilon = \frac{1}{n} \left( \frac{1}{EIE} - 1 \right) \cdot 1000, \quad (2)$$

where  $n$  represents the number of atoms of the same element in a molecule (?? ) that have been isotopically substituted. EIE and  $\varepsilon$  have been calculated in the developing version of

the open source program isoC.<sup>44</sup> Enrichment factor  $\varepsilon$  is used along this work for consistency with experimental data.

A decomposition energy analysis is performed in order to obtain an insight into compounds interactions strength and correctly identify patters between FHVA and isotope effects. Clusters were divided in single molecules (four per cluster) and all arranges (six) of possible dimers were promptly formed, consequently, interaction energy  $E_{\text{int}}$  for dimers were calculated using the symmetry-adapted perturbation theory (SAPT).<sup>45</sup> Within the so-called supermolecular approach that SAPT follows, interaction energy  $E_{\text{int}}$  of a system typically consisting of two separable subsystems  $A$  and  $B$  is defined as

$$E_{\text{int}} = E_{\text{AB}} - E_{\text{A}} - E_{\text{B}}. \quad (3)$$

In parallel, the SAPT interaction energy can be further expanded and decomposed into four physically meaningful components *i.e.* electrostatic, exchange, induction, and dispersion yielding

$$E_{\text{int}} = E_{\text{elst}} + E_{\text{exch}} + E_{\text{ind}} + E_{\text{disp}}, \quad (4)$$

where  $E_{\text{elst}}$  is the electrostatic component,  $E_{\text{exch}}$  represents the exchange term,  $E_{\text{ind}}$  gives the inductions component, and  $E_{\text{disp}}$  indicates the dispersion term of interaction energy. Owing to the relative compact size of the studied molecules, a large basis set (Dunning’s correlation-consistent augmented triple) along with accurate higher-order SAPT (SAPT+2) with coupled-cluster doubles (CCD) treatment of dispersion and supermolecular MP2 interaction energy ( $\delta\text{MP2}$ )<sup>40,41</sup> is utilised for  $E_{\text{int}}$  accurate calculation. Interaction energies were calculated in the standard release of PSI4 software package (version 1.3.2).<sup>46</sup>

Complementarity to SAPT analysis, non-covalent interactions were visualised and meticulously studied by means of independent gradient model (IGM).<sup>47</sup> Intermolecular interactions described by the density gradient as implemented in the stable release of Multiwfn package software (version 3.6) was used.<sup>48</sup>

## Results and discussion

Table 2 contains average root-mean-square deviation (RMDS) of aligned atomic positions from successfully optimised geometries that also were confirmed to be stationary points without negative frequencies. Although all five BB clusters were geometrically optimised,

**Table 2: Root-mean-square deviation of atomic positions for geometrically optimised clusters (CFC, DBM, EtOH, MeOH, and TCM) at  $\omega$ B97X-V/aug-cc-pvdz and  $\omega$ B97X-V/aug-cc-pvtz levels of theory.**

Compound	Atoms compared	RMSD [ $\text{\AA}$ ]	
		aug-cc-pvdz	aug-cc-pvtz
CFC	all	2.41	2.24
CFC	C	1.82	1.85
DBM	all	1.94	1.87
DBM	C	1.51	1.46
DBM	Br	2.13	2.14
EtOH	all	1.95	2.00
EtOH	C	1.74	1.78
EtOH	O	1.62	1.39
MeOH	all	1.90	1.87
MeOH	C	1.74	1.73
MeOH	O	1.33	1.27
TCM	all	2.00	1.90
TCM	C	1.48	1.34

stationary points could not be validated from FHVA calculations as those exceeded the computational time limit. It is important to realise that generally speaking, clusters are heterogeneous and possess relatively large RMSD, indicating that VIE and VPIE predictions are obtained to several configurations of the PES. The increase of the basis from aug-cc-pvdz to aug-cc-pvtz, in general only slightly decrease the RMSD.

Two pair of clusters, ones in case of EtOH (EtOH-1 and EtOH-2) and MeOH (MeOH-3 and MeOH-4), resulted in identical atomic positions, which can be interpreted as likely abundant configuration within the PES. Another key point from RMSD is its minimal value for oxygen atoms in EtOH and MeOH, probably owing to their relevance in the formation of hydrogen bonds (HB). It is well recognised that given compounds mainly interact *via*

hydrogen bonding, a weak non-covalent interaction, thus it is reasonably expected that oxygen atomic positions would not vary or at least not as halogen atoms, which non-covalent interactions are significantly weaker.

Average VIEs for studied compounds are given in table 3. Isotope effect results for CFC

**Table 3: VIEs ( $\varepsilon$  ‰) predicted at standard conditions for trichlorofluoromethane, dibromomethane, ethanol, methanol, and trichloromethane, at  $\omega$ B97X-V/aug-cc-pvdz level of theory.**

Compound	isotope	$\varepsilon$	Exp.
CFC	$^{13}\text{C}$	0.64	1.7 <sup>1</sup>
DBM	$^{81}\text{Br}$	-1.74	-0.8±0.1 <sup>2</sup>
DBM	$^{13}\text{C}$	-1.99	0.6±0.2 <sup>2</sup>
EtOH	$^{13}\text{C}_1$	-1.26	-6.1 <sup>3</sup>
EtOH	$^{13}\text{C}_2$	0.56	-2.6 <sup>3</sup>
MeOH	$^{13}\text{C}$	1.04	-6.5 <sup>3</sup>
TCM	$^{13}\text{C}$	0.16	1.2 <sup>1</sup>

<sup>1</sup>Ref. 3.

<sup>2</sup>Ref. 49.

<sup>3</sup>Ref. 5 by passive evaporation.

produce a qualitatively match with respect to experimental data,<sup>3</sup> however it is underestimated. Small mean standard deviation (STD) from position-specific isotope effects (see table S1 of supplementary information) in CFC along with RMSD, indicate that although cluster atomic positions differ appreciably from each other, this variety in the PES does not affect the final prediction.

$^{81}\text{Br}$  isotope effect for DBM is overestimated, while  $^{13}\text{C}$  is rightly predicted as normal, but its magnitude is three times larger than the one from experimental data. The last from the group of halogenated compounds is TCM, which  $^{13}\text{C}$  isotope effect is only predicted qualitatively, *i.e.* an inverse isotope effect is predicted, however its value is a factor of magnitude underestimated.

Average position-specific isotope effect for  $^{13}\text{C}_1$  in EtOH is underestimated, whereas  $^{13}\text{C}_2$  is not predicted qualitatively either quantitatively. Nevertheless, it is worth mentioning that position-specific isotope effects values for  $^{13}\text{C}_2$  were in their vast majority close to zero, with

only a couple being larger than one. Thus, if  $^{13}\text{C}_2$  is recalculated with the position-specific values closer to zero, the predicted isotope effect respectively becomes 0.27‰. The apparent reason behind such particularly differences in the positions-specific magnitudes is diligently studied and explained in the next section (??).

According to our compounds scheme, the second carbon position in EtOH and the carbon position in MeOH are similar, as both atoms are bonded to OH, therefore it is interesting to characterise how different or similar their position-specific isotope effects are. Predicted  $^{13}\text{C}$  in MeOH is a moderate inverse effect (1.04‰), contrary to the considerable normal effect observed in the experimental data. The STD for  $^{13}\text{C}$  in MeOH reveals that computed VIE fluctuates along a broad range of values ( $\pm 3.9$ ), therefore, first it is necessary to minimise the STD in order to infer further conclusions.

The expansion of the basis set to aug-cc-pvtz for the calculation of VIEs provide a drastic change in the predicted values of DBM and MeOH (table 4), the rest of the compounds did not undergo relevant changes. In general,  $^{81}\text{Br}$  and  $^{13}\text{C}$  isotope effects for DBM were diminished at least by a factor of magnitude, thus  $^{81}\text{Br}$  passed from -1.17 to -0.02‰ and  $^{13}\text{C}$  from -1.99 to -0.17‰. For  $^{13}\text{C}$  in MeOH, it is worth noting that although the calculated isotope effect agrees qualitatively with experimental results, *i.e.* predicted value reflects a normal isotope effect, its magnitude is severely underestimated. Additionally, it is observed that in general the STDs (see table S2 of supplementary information) have become smaller, especially in the case of MeOH.

In conjunction with VIEs, VPIE were calculated for compounds with present experimental data.  $^{13}\text{C}$  VPIE for EtOH and MeOH at  $\omega\text{B97X-V/aug-cc-pvdz}$  and  $\omega\text{B97X-V/aug-cc-pvtz}$  levels of theory are given in the tables 5 and 6, respectively. Contrary to experimental results, predicted VPIE are notoriously unaffected by the temperature change. In the case of  $^{13}\text{C}_2$  for EtOH and  $^{13}\text{C}$  in MeOH, predicted values are closer to experimental data, specially  $^{13}\text{C}_2$ . However, it must be recalled that it is precisely the position-specific isotope effect for carbon atom bonded OH, the one that reflected large STD.

**Table 4:** VIEs ( $\varepsilon$  ‰) predicted at standard conditions for trichlorofluoromethane, dibromomethane, ethanol, methanol, and trichloromethane, at  $\omega$ B97X-V/aug-cc-pvtz level of theory.

Compound	isotope	$\varepsilon$	Exp.
CFC	$^{12}\text{C}$	0.64	1.7 <sup>1</sup>
DBM	$^{81}\text{Br}$	-0.02	-0.8±0.1 <sup>2</sup>
DBM	$^{13}\text{C}$	-0.17	0.6±0.2 <sup>2</sup>
EtOH	$^{13}\text{C}_1$	-1.18	-6.1 <sup>3</sup>
EtOH	$^{13}\text{C}_2$	0.47	-2.6 <sup>3</sup>
MeOH	$^{13}\text{C}$	-0.13	-6.5 <sup>3</sup>
TCM	$^{13}\text{C}$	0.09	1.2 <sup>1</sup>

<sup>1</sup>Ref. 3.

<sup>2</sup>Ref. 49.

<sup>3</sup>Ref. 5 by passive evaporation.

**Table 5:** VPIEs ( $\varepsilon$  ‰) for ethanol, and methanol, predicted at  $\omega$ B97X-V/aug-cc-pvdz level of theory.

Compound	isotope	$\varepsilon$	Exp.
EtOH	$^{13}\text{C}_1$	-0.99	1.1 <sup>1</sup>
EtOH	$^{13}\text{C}_2$	0.47	0.3 <sup>1</sup>
MeOH	$^{13}\text{C}$	0.93	0.5 <sup>1</sup>

<sup>1</sup>Ref. 5 by distillation.

**Table 6:** VPIEs ( $\varepsilon$  ‰) for ethanol, and methanol, predicted at  $\omega$ B97X-V/aug-cc-pvtz level of theory.

Compound	isotope	$\varepsilon$	Exp.
EtOH	$^{13}\text{C}_1$	-0.94	1.1 <sup>1</sup>
EtOH	$^{13}\text{C}_2$	-0.40	0.3 <sup>1</sup>
MeOH	$^{13}\text{C}$	-0.14	0.5 <sup>1</sup>

<sup>1</sup>Ref. 5 by distillation.

## Effects from Hessian matrix approach

Table 8 contains VIEs predictions for studies systems at  $\omega$ B97X-V/aug-cc-pvdz level of theory. Predominantly, numerical calculations reveal that unless molecules in the cluster are

**Table 7: VIEs ( $\varepsilon$  %) predicted from partial Hessian vibrational analysis at standard conditions for bromobenzene, trichlorofluoromethane, dibromomethane, ethanol, methanol, and trichloromethane, at  $\omega$ B97X-V/aug-cc-pvdz level of theory.**

Compound	isotope	$\varepsilon$	Exp.
BB	$^{81}\text{Br}$	0.04	$-0.9 \pm 0.2^1$
BB	$^{13}\text{C}$	0.11	$-0.4 \pm 0.1^1$
CFC	$^{12}\text{C}$	0.63	1.7 <sup>2</sup>
EtOH	$^{13}\text{C}_1$	-0.79	-6.1 <sup>3</sup>
EtOH	$^{13}\text{C}_2$	1.08	-2.6 <sup>3</sup>
MeOH	$^{13}\text{C}$	0.87	-6.5 <sup>3</sup>
TCM	$^{13}\text{C}$	0.19	1.2 <sup>2</sup>

<sup>1</sup>Ref. 49.

<sup>2</sup>Ref. 3.

<sup>3</sup>Ref. 5 by passive evaporation.

interacting directly *via* hydrogen bond, frequencies are unaffected, hence allowing practically identical isotope effects as calculated with FHVA. Given result is highly valuable and promising, as it naturally allows us to accurately calculate with confidence  $^{81}\text{Br}$  and  $^{13}\text{C}$  isotope effects in BB, for which FHVA could not be computed owing to computational time limits. It is worth mentioning that computational time was decreased by 75 % in average by employing PHVA, as compared to FHVA.

It must be remembered that within the concept of the reduced partition function ratio (RPFR) by the Bigeleisen-Mayer approximation,<sup>8</sup> it is equally possible to describe the isotope effect as the product of three factors, i) the product factor (PF), which contains molecular masses and moments of inertia, ii) the excitation factor (EXP), which introduces a correction for excited molecules, and iii) the zero-point energy contribution (ZPE) factor, which describes the zero-point energy differences for each of the vibrational modes.<sup>9,50</sup> As a rule, PF tends to remain a minor factor, as well as EXP which vanishes at elevated temper-

atures, therefore, ZPE represents the factor that typically determines the direction of the isotope effect (normal or inverse).

Given that only one molecule in the cluster was active during PHVA, the PF in all performed calculations is close to one. The effect of PHVA in the remaining terms (EXP and ZPE) was studied by calculating those directly within isoC.<sup>44</sup> For direct reference TCM and CFC from FHVA and PHVA were used, as precisely named systems did not present differences in the averaged VIE. There were not found relevant patterns for ZPE from PHVA. The only observed characteristic was that this term seemed to fluctuate in a convenient way to properly compensate the fact that EXC is always larger than its respective term from FHVA, thus ZPE values from PHVA were shifted. This observation is clearly evident when statistical parameters such as STD, skewness and kurtosis were compared between PHVA and FHVA, indicating close or identical values.

## **Role of non-covalent interactions in the prediction of isotope effects**

Total interaction energies *via* SAPT along with visualisation of non-covalent interactions from IGM analyses, was used in order to characterise the magnitude of interactions in the first cluster of each compound optimised at the  $\omega$ B97X-V/aug-cc-pvdz level of theory (see fig. S1 in supplementary information).

As each cluster consists precisely of four molecules, a total of six unique dimer arrangements can be formed, thus for instance to ethanol cluster the following dimers were formed: 1<sup>st</sup> EtOH molecule with 2<sup>nd</sup> EtOH molecule, 1<sup>st</sup> EtOH molecule with 3<sup>rd</sup> EtOH molecule, 1<sup>st</sup> EtOH molecule with 4<sup>th</sup> EtOH molecule, 2<sup>nd</sup> EtOH molecule with 3<sup>rd</sup> EtOH molecule, 2<sup>nd</sup> EtOH molecule with 4<sup>th</sup> EtOH molecule, and 3<sup>rd</sup> EtOH molecule with 4<sup>th</sup> EtOH molecule. Figure 1 shows bar plots with total interaction energies per dimer of each studied compound.

Results demonstrate that CFC possesses the weakest interactions among studied compounds. In increasing order, CFC is followed by TCM, DBM, BB, MeOH, and EtOH.

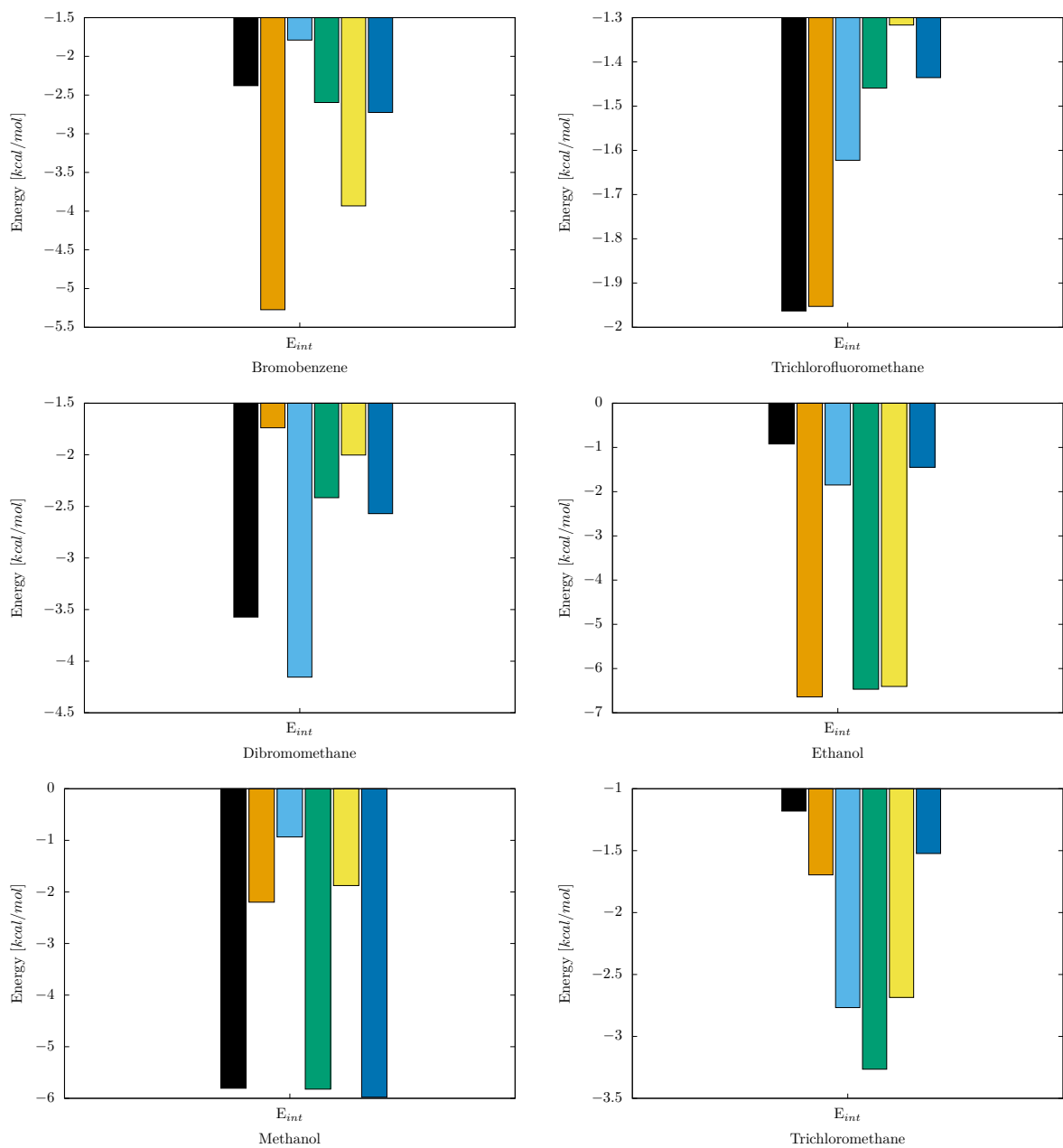


Figure 1: Interaction energy for studied compounds of cluster one optimised at  $\omega$ B97x-V/aug-cc-pvdz. Each colour bar indicates one dimer combination (six per system), within a four molecule cluster.

Moreover, given order correlates with obtained reduced density gradients of intermolecular interactions from IGM analysis (see fig. S2 in supplementary information).

Although from SAPT calculations BB does not seem to typically reflect relatively strong interaction energies, the orange bar stands out over the rest. A comprehensive analysis of given result indicates it corresponds to a  $\pi$ - $\pi$  stacking (parallel displaced), which is promptly confirmed after properly comparing dispersion and electrostatics components from the interaction energy decomposition (see fig. S3 in supplementary information).

The three bars (orange, green, and yellow) are prominent in EtOH SAPT analysis and precisely correspond to the formed hydrogen bonds. Average interaction energy of hydrogen bonds is  $6.5 \text{ kcal mol}^{-1}$ , which match perfectly Vargas-Caamal’s average from high level of theory calculations.<sup>51</sup> Remaining dimer interactions are relatively weak and principally raise from electrostatic interactions. As expected, MeOH interaction energies faithfully reflect a similar pattern with EtOH, *i.e.* interaction mainly *via* electrostatics, three dimers displaying potent attractive interactions (hydrogen bonding) and other three significantly weaker.

TCM interaction energies are the second weakest after CFC. Moreover, similar to CFC, BB and DBM intermolecular interactions are predominantly dispersion driven (see fig. S3 in supplementary information).

Among compounds DBM is genuinely interesting as SAPT analysis shows that it is the only compound among the studied ones, which interactions energies are proportionally distributed between electrostatics and dispersion (mixed type<sup>52</sup>). Furthermore, only in the case of DBM the induction component of the interaction energies is positive although weak in magnitude, therefore indicating a meagre DBM polarisation.

Other set of SAPT calculations were performed using optimised atomic positions of the fourth cluster at the  $\omega$ B97X-V/aug-cc-pvtz level of theory, in order to i) establish whether consistent patterns observed in the previously studied cluster prevail in other cluster, and ii) accurately identify general energetic changes with the increase of the basis set. Results (table 8) suggest that in average minimal alterations in interactions energies are perceived.

Consequently, interaction energy components (electrostatics, exchange, induction, and dis-

**Table 8: Average interaction energies from SAPT analysis for geometrically optimised clusters (BB, CFC, DBM, EtOH, MeOH, and TCM) at  $\omega$ B97X-V/aug-cc-pvdz and  $\omega$ B97X-V/aug-cc-pvdz levels of theory.**

Compound	Ave. $E_{\text{int}}$ [kcal mol <sup>-1</sup> ]	
	aug-cc-pvdz	aug-cc-pvtz
BB	-3.12	-2.98
CFC	-1.63	-1.65
DBM	-2.74	-2.25
EtOH	-3.96	-3.85
MeOH	-3.77	-3.52
TCM	-2.19	-2.21

persion) are seemingly unaffected (see figs. S4 and S5 in supplementary information). Plausible explanation to the dramatic transformation in the prediction of <sup>81</sup>Br and <sup>13</sup>C VIEs for DBM are sought in the SAPT results. Not surprisingly, DBM interaction energies are precisely the ones that comparatively change the most. We notice that distinctively one of the dimers does not possess any kind of intermolecular interaction, which results in an average weaker intermolecular interaction.

Visualisation of intermolecular interactions by IGM analysis are provided in fig. 2. BGR colour space is used for representing characteristic interactions, thus blue implies strong attractive forces, green alludes van der Waals interactions, and red determines strong repulsive forces. Br atoms in BB do seem to occupy an active role in the interactions, which is most likely one of the possible reason why there were not VIEs in the PHVA. Overall weak interactions from SAPT analysis correlates with IGM picture of intermolecular interactions seen in CFC and TCM.

DBM demonstrates abundant interactions (van der Waals forces in green). However, this representation changes upon increasing the basis set. It is observed that the general extension of van der Waals forces is substantially diminished (see fig. S6 in supplementary information), therefore enlarging the compelling evidence that points the weakening on interatomic

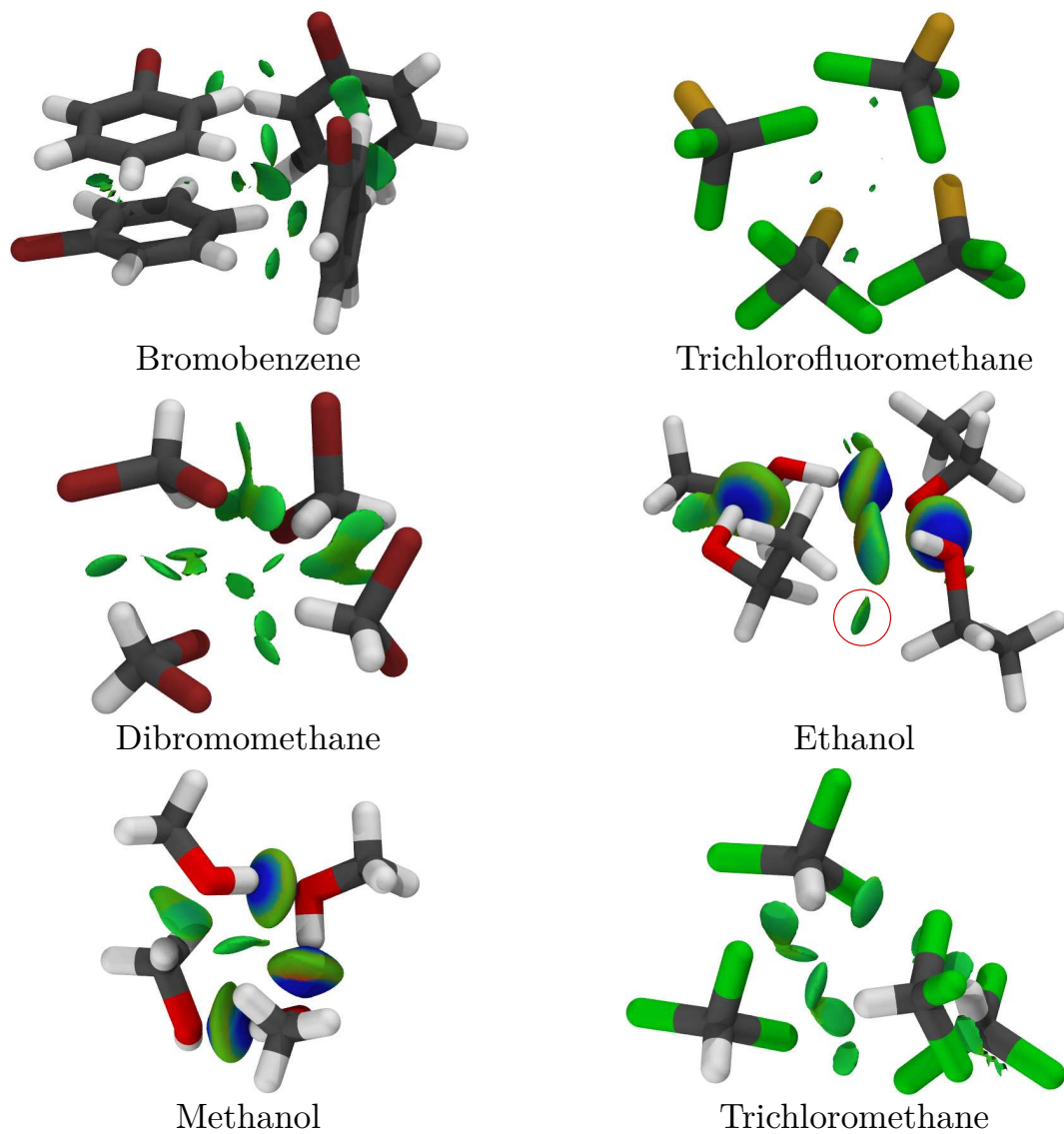


Figure 2: Visualisation of intermolecular interactions from IGM analysis. BGR colour space describes intermolecular interactions, where strong attraction is highlighted in blue, van der Waals interactions are shown in green, and strong repulsion is displayed red.

interactions, as the key reason for the immoderate change of isotope effects prediction.

Using IGM for EtOH cluster, we detected that apparently a moderate van der Waals force (red circle in fig. 2) is responsible for the large STD during the calculation of  $^{13}\text{C}_2$  VIE. Given intermolecular interaction was only observed over/around  $\text{C}_2$  atomic positions that, correspondingly, after being isotopically substituted to  $^{13}\text{C}$ , exhibited relative large magnitudes ( $\approx 1.0\%$ ). Because EtOH molecules interact massively *via* hydrogen bonds, it is unreasonable to dismiss the fact that the intensity or lack of hydrogen bonds might be equally contributing to the overall STD. Which is precisely the case of MeOH cluster.  $^{13}\text{C}$  isotope effects for MeOH display the largest STD among the studied compounds at the  $\omega\text{B97X-V/aug-cc-pvdz}$  level of theory, and there are not systematic patterns between position-specific isotope effects, SAPT, and IGM analysis that permit the proper identification of the large STD cause. Similarly IGM analysis on optimised atomic positions at the  $\omega\text{B97X-V/aug-cc-pvtz}$  level of theory (see fig. S7 in supplementary information) does not provide straightforward insight into the issue.

## Conclusions

We have calculated average volatilisation-pressure isotope effects for trichlorofluoromethane, dibromomethane, ethanol, methanol, and trichloromethane from full Hessian vibrational analysis at the  $\omega\text{B97X-V/aug-cc-pvdz}$  level of theory. Generally, isotope effects were predicted in qualitative agreement with experimental results. Isotope effects calculations with a larger basis set (aug-cc-pvtz) exhibit smaller standard deviation errors, and in most of the cases their magnitudes did not change appreciably compared to the smaller basis set (aug-cc-pvdz) results. Vapour-pressure isotope effects were in better agreement with experimental data.

As for equilibrium isotope effects calculation, partial Hessian vibrational analysis<sup>28,31</sup> provides a robust, computational inexpensive and easy approach for their accurate calculation.

We observed that unless intermolecular interactions of the studied compound are carried out via *via* hydrogen bonds, accuracy of predicted isotope effects is uncompromised and equals isotope effect magnitudes from full Hessian vibrational analyses. It is substantial to note that using partial Hessian vibrational analysis, average computational time was reduced by a 75% in comparison to full Hessian vibrational analysis.

Furthermore, we noticed that the product factor and the excitation factor of the reduced partition function ratio by the Bigeleisen-Mayer approximation,<sup>8</sup> are almost one ( $\approx 0.999$ ) in the vast majority of cases. Under those circumstances, the zero-point energy contribution from partial Hessian vibrational analysis shifts in order to equal predicted isotope effects from full Hessian vibrational analysis. With this in mind, we were able to predict  $^{13}\text{C}$  and  $^{81}\text{Br}$  isotope effects in bromobenzene, as it was not possible with full Hessian vibrational analysis due to computational time limitations.

The symmetry-adapted perturbation theory combined with independent gradient model has undoubtedly resulted in a successful scheme in order to appreciate qualitatively and quantitatively the consequences of intermolecular interactions in the calculation of equilibrium isotope effects. Thus for instance, the severe difference in the predicted values of  $^{13}\text{C}$  and  $^{81}\text{Br}$  isotope effects for dibromomethane when the size of basis set is increased, can be satisfactorily explained by the general reduction of intermolecular interactions. Although the present scheme was properly employed for studying all compounds, it is important to mention that owing to the relative strong interaction of hydrogen bonding systems (ethanol and methanol), comprehensible and straightforward assessment by independent gradient model becomes laborious. Because visually more interactions come in direct contact, which makes difficult to accurately distinguish interactions between specific atoms or regions. For the purpose of overcoming that inconvenience, we recommend to complementary use other more flexible visualisation techniques such as the electron localisation function (ELF)<sup>53</sup> and atoms in molecules (AIM).<sup>54</sup>

It is worthwhile to mention that the employed method for studying intermolecular in-

teractions requires the use of high level of theory methods, or at least rigorous functionals within KS DFT, in order to reproduce compound atomic positions exact or relatively close to experimental data. Poor reproduction of atoms interaction in a cluster will undoubtedly lead to misleading interpretations of the PES, therefore we recommend well tested and benchmarked<sup>15</sup> KS DFT functionals such as  $\omega$ B97X-V.

## Acknowledgments

This work was supported by the National Science Centre in Poland (Sonata BIS grant UMO-2014/14/E/ST4/00041) and in part by PLGrid Infrastructure (Poland).

## References

- (1) Julien, M.; Hoöhener, P.; Robins, R. J.; Parinet, J.; Remaud, G. S. Position-Specific <sup>13</sup>C Fractionation during Liquid–Vapor Transition Correlated to the Strength of Inter-molecular Interaction in the Liquid Phase. *The Journal of Physical Chemistry B* **2017**, *121*, 5810–5817.
- (2) Julien, M.; Parinet, J.; Nun, P.; Bayle, K.; Hhener, P.; Robins, R. J.; Remaud, G. S. Fractionation in position-specific isotope composition during vaporization of environmental pollutants measured with isotope ratio monitoring by <sup>13</sup>C nuclear magnetic resonance spectrometry. *Environmental Pollution* **2015**, *205*, 299–306.
- (3) Horst, A.; Lacrampe-Couloume, G.; Lollar, B. S. Vapor Pressure Isotope Effects in Halogenated Organic Compounds and Alcohols Dissolved in Water. *Analytical Chemistry* **2016**, *88*, 12066–12071.
- (4) Heckel, B.; Phillips, E.; Edwards, E.; Lollar, B. S.; Elsner, M.; Manefield, M. J.; Lee, M. Reductive Dehalogenation of Trichloromethane by Two Different Dehalobacter restric-

- tusStrains Reveal Opposing Dual Element Isotope Effects. *Environmental Science & Technology* **2019**, *53*, 2332–2343.
- (5) Julien, M.; Nun, P.; Robins, R. J.; Remaud, G. S.; Parinet, J.; Höhener, P. Insights into Mechanistic Models for Evaporation of Organic Liquids in the Environment Obtained by Position-Specific Carbon Isotope Analysis. *Environmental Science & Technology* **2015**, *49*, 12782–12788.
- (6) Kopinke, F.-D.; Georgi, A. Comment on Vapor Pressure Isotope Effects in Halogenated Organic Compounds and Alcohols Dissolved in Water. *Analytical Chemistry* **2017**, *89*, 10637–10638.
- (7) Jancso, G.; Hook, W. A. V. Condensed phase isotope effects. *Chemical Reviews* **1974**, *74*, 689–750.
- (8) Bigeleisen, J.; Mayer, M. G. Calculation of Equilibrium Constants for Isotopic Exchange Reactions. *The Journal of Chemical Physics* **1947**, *15*, 261–267.
- (9) Wolfsberg, M.; Hook, W. A.; Paneth, P.; Rebelo, L. P. N. *Isotope Effects*; Springer Netherlands: Dordrecht, 2009.
- (10) Kohn, W.; Sham, L. J. Self-Consistent Equations Including Exchange and Correlation Effects. *Physical Review* **1965**, *140*, 1133–1138.
- (11) Vosko, S. H.; Wilk, L.; Nusair, M. Accurate spin-dependent electron liquid correlation energies for local spin density calculations: a critical analysis. *Canadian Journal of Physics* **1980**, *58*, 1200–1211.
- (12) Lee, C.; Yang, W.; Parr, R. G. Development of the Colle-Salvetti correlation-energy formula into a functional of the electron density. *Physical Review B* **1988**, *37*, 785–789.
- (13) Becke, A. D. Density-functional thermochemistry. III. The role of exact exchange. *The Journal of Chemical Physics* **1993**, *98*, 5648–5652.

- (14) Stephens, P. J.; Devlin, F. J.; Chabalowski, C. F.; Frisch, M. J. Ab Initio Calculation of Vibrational Absorption and Circular Dichroism Spectra Using Density Functional Force Fields. *The Journal of Physical Chemistry* **1994**, *98*, 11623–11627.
- (15) Goerigk, L.; Hansen, A.; Bauer, C.; Ehrlich, S.; Najibi, A.; Grimme, S. A look at the density functional theory zoo with the advanced GMTKN55 database for general main group thermochemistry, kinetics and noncovalent interactions. *Physical Chemistry Chemical Physics* **2017**, *19*, 32184–32215.
- (16) Adamo, C.; Barone, V. Toward reliable density functional methods without adjustable parameters: The PBE0 model. *The Journal of Chemical Physics* **1999**, *110*, 6158–6170.
- (17) Ernzerhof, M.; Scuseria, G. E. Assessment of the Perdew–Burke–Ernzerhof exchange–correlation functional. *The Journal of Chemical Physics* **1999**, *110*, 5029–5036.
- (18) Adamo, C.; Barone, V. Exchange functionals with improved long-range behavior and adiabatic connection methods without adjustable parameters: The mPW and mPW1PW models. *The Journal of Chemical Physics* **1998**, *108*, 664–675.
- (19) Oi, T.; Mitome, R.; Yanase, S. Hydrogen and Carbon Vapour Pressure Isotope Effects in Liquid Fluoroform Studied by Density Functional Theory. *Zeitschrift für Naturforschung A* **2017**, *72*, 061701–061701.
- (20) Yanase, S.; Oi, T. Vapor pressure isotope effects in methyl fluoride studied by density functional theory. *Chemical Physics Letters* **2007**, *440*, 19–23.
- (21) Pulay, P. Ab initio calculation of force constants and equilibrium geometries in polyatomic molecules. *Molecular Physics* **1969**, *17*, 197–204.
- (22) McIver, J. W.; Komornicki, A. Structure of transition states in organic reactions. General theory and an application to the cyclobutene-butadiene isomerization using

- a semiempirical molecular orbital method. *Journal of the American Chemical Society* **1972**, *94*, 2625–2633.
- (23) Rahalkar, A. P.; Ganesh, V.; Gadre, S. R. Enabling ab initio Hessian and frequency calculations of large molecules. *The Journal of Chemical Physics* **2008**, *129*, 234101.
- (24) Sharada, S. M.; Bell, A. T.; Head-Gordon, M. A finite difference Davidson procedure to sidestep full ab initio hessian calculation: Application to characterization of stationary points and transition state searches. *The Journal of Chemical Physics* **2014**, *140*, 164115.
- (25) Yamamoto, S.; Bouř, P. *Frontiers of Quantum Chemistry*; Springer Singapore, 2017; pp 181–197.
- (26) Yang, T.; Berry, J. F. Numerical Nuclear Second Derivatives on a Computing Grid: Enabling and Accelerating Frequency Calculations on Complex Molecular Systems. *Journal of Chemical Theory and Computation* **2018**, *14*, 3459–3467.
- (27) Pascale, F.; Zicovich-Wilson, C. M.; Gejo, F. L.; Civalleri, B.; Orlando, R.; Dovesi, R. The calculation of the vibrational frequencies of crystalline compounds and its implementation in the CRYSTAL code. *Journal of Computational Chemistry* **2004**, *25*, 888–897.
- (28) Head, J. D. Computation of vibrational frequencies for adsorbates on surfaces. *International Journal of Quantum Chemistry* **1997**, *65*, 827–838.
- (29) Head, J. D.; Shi, Y. Characterization of Fermi resonances in adsorbate vibrational spectra using cluster calculations: Methoxy adsorption on Al(111) and Cu(111). *International Journal of Quantum Chemistry* **1999**, *75*, 815–820.
- (30) Sae-Heng, P.; Tantirungrotechai, J.; Tantirungrotechai, Y. Scale Factors for Carbonyl

- Vibrational Frequencies: A Study of Partial Hessian Approximation. *Chiang Mai Journal of Science* **2018**, *45*, 2797–2808.
- (31) Besley, N. A.; Bryan, J. A. Partial Hessian Vibrational Analysis of Organic Molecules Adsorbed on Si(100). *The Journal of Physical Chemistry C* **2008**, *112*, 4308–4314.
- (32) Li, H.; Jensen, J. H. Partial Hessian vibrational analysis: the localization of the molecular vibrational energy and entropy. *Theoretical Chemistry Accounts: Theory, Computation, and Modeling (Theoretica Chimica Acta)* **2002**, *107*, 211–219.
- (33) Yuan, J. Reduced Partition Function Ratio in the Frequency Complex Plane: A Mathematical Approach. *Open Journal of Geology* **2014**, *04*, 654–664.
- (34) Rustad, J. R.; Zarzycki, P. Calculation of site-specific carbon-isotope fractionation in pedogenic oxide minerals. *Proceedings of the National Academy of Sciences* **2008**, *105*, 10297–10301.
- (35) Plimpton, S. Fast Parallel Algorithms for Short-Range Molecular Dynamics. *Journal of Computational Physics* **1995**, *117*, 1–19.
- (36) Jorgensen, W. L.; Maxwell, D. S.; Tirado-Rives, J. Development and Testing of the OPLS All-Atom Force Field on Conformational Energetics and Properties of Organic Liquids. *Journal of the American Chemical Society* **1996**, *118*, 11225–11236.
- (37) Jorgensen, W. L.; Tirado-Rives, J. The OPLS [optimized potentials for liquid simulations] potential functions for proteins, energy minimizations for crystals of cyclic peptides and crambin. *Journal of the American Chemical Society* **1988**, *110*, 1657–1666.
- (38) Dodda, L. S.; Cabeza de Vaca, I.; Tirado-Rives, J.; Jorgensen, W. L. LigParGen web server: an automatic OPLS-AA parameter generator for organic ligands. *Nucleic Acids Research* **2017**, *45*, W331–W336.

- (39) Mardirossian, N.; Head-Gordon, M.  $\omega$ B97X-V: A 10-parameter, range-separated hybrid, generalized gradient approximation density functional with nonlocal correlation, designed by a survival-of-the-fittest strategy. *Physical Chemistry Chemical Physics* **2014**, *16*, 9904.
- (40) Parrish, R. M.; Hohenstein, E. G.; Sherrill, C. D. Tractability gains in symmetry-adapted perturbation theory including coupled double excitations: CCD+ST(CCD) dispersion with natural orbital truncations. *The Journal of Chemical Physics* **2013**, *139*, 174102.
- (41) Parker, T. M.; Burns, L. A.; Parrish, R. M.; Ryno, A. G.; Sherrill, C. D. Levels of symmetry adapted perturbation theory (SAPT). I. Efficiency and performance for interaction energies. *The Journal of Chemical Physics* **2014**, *140*, 094106.
- (42) Dasgupta, S.; Herbert, J. M. Standard grids for high-precision integration of modern density functionals: SG-2 and SG-3. *Journal of Computational Chemistry* **2017**, *38*, 869–882.
- (43) Shao, Y.; Gan, Z.; Epifanovsky, E.; Gilbert, A. T.; Wormit, M.; Kussmann, J.; Lange, A. W.; Behn, A.; Deng, J.; Feng, X. et al. Advances in molecular quantum chemistry contained in the Q-Chem 4 program package. *Molecular Physics* **2014**, *113*, 184–215.
- (44) Vasquez, L. isoC. 2019.
- (45) Jeziorski, B.; Moszynski, R.; Szalewicz, K. Perturbation Theory Approach to Intermolecular Potential Energy Surfaces of van der Waals Complexes. *Chemical Reviews* **1994**, *94*, 1887–1930.
- (46) Parrish, R. M.; Burns, L. A.; Smith, D. G. A.; Simmonett, A. C.; DePrince, A. E.; Hohenstein, E. G.; Bozkaya, U.; Sokolov, A. Y.; Remigio, R. D.; Richard, R. M. et al.

- Psi4 1.1: An Open-Source Electronic Structure Program Emphasizing Automation, Advanced Libraries, and Interoperability. *Journal of Chemical Theory and Computation* **2017**, *13*, 3185–3197.
- (47) Lefebvre, C.; Khartabil, H.; Boisson, J.-C.; Contreras-García, J.; Piquemal, J.-P.; Hénon, E. The Independent Gradient Model: A New Approach for Probing Strong and Weak Interactions in Molecules from Wave Function Calculations. *ChemPhysChem* **2018**, *19*, 724–735.
- (48) Lu, T.; Chen, F. Multiwfn: A multifunctional wavefunction analyzer. *Journal of Computational Chemistry* **2011**, *33*, 580–592.
- (49) Vasquez, L.; Rostkowski, M.; Gelman, F.; Dybala-Defratyka, A. Can Path Integral Molecular Dynamics Make a Good Approximation for Vapor Pressure Isotope Effects Prediction for Organic Solvents? A Comparison to ONIOM QM/MM and QM Cluster Calculation. *The Journal of Physical Chemistry B* **2018**, *122*, 7353–7364.
- (50) Van Hook, W. Isotope effects in chemistry. *Nukleonika -Original Edition-* **2011**, *56*, 217–240.
- (51) Vargas-Caamal, A.; Ortiz-Chi, F.; Moreno, D.; Restrepo, A.; Merino, G.; Cabellos, J. L. The rich and complex potential energy surface of the ethanol dimer. *Theoretical Chemistry Accounts* **2015**, *134*.
- (52) Řezáč, J.; Riley, K. E.; Hobza, P. S66: A Well-balanced Database of Benchmark Interaction Energies Relevant to Biomolecular Structures. *Journal of Chemical Theory and Computation* **2011**, *7*, 2427–2438.
- (53) Becke, A. D.; Edgecombe, K. E. A simple measure of electron localization in atomic and molecular systems. *The Journal of Chemical Physics* **1990**, *92*, 5397–5403.

- (54) KUMAR, P. S. V.; RAGHAVENDRA, V.; SUBRAMANIAN, V. Bader's Theory of Atoms in Molecules (AIM) and its Applications to Chemical Bonding. *Journal of Chemical Sciences* **2016**, *128*, 1527–1536.

**Supplementary Material**

**Partial Hessian vibrational analysis: vapour  
pressure isotope effects and their relation with  
non-covalent interactions**

Luis Vasquez\*

*Institute of Applied Radiation Chemistry, Lodz University of Technology, Żeromskiego 116,  
Łódź 90-914, Poland*

E-mail: [luis.vasquez@dokt.p.lodz.pl](mailto:luis.vasquez@dokt.p.lodz.pl)

**Table S1:** VPIEs ( $\varepsilon$  ‰) predicted on evaporation using aug-cc-pvdz basis set for trichlorofluoromethane, dibromomethane, ethanol, methanol, and trichloromethane.

Compound	<i>isotope</i>	$\varepsilon$	STD	Exp.
CFC	$^{12}\text{C}$	0.6362	0.1005	1.7 <sup>1</sup>
DBM	$^{81}\text{Br}$	-1.7366	0.0329	-0.80.1 <sup>2</sup>
DBM	$^{13}\text{C}$	-1.9926	0.2431	0.6 <sup>2</sup>
EtOH	$^{13}\text{C}_1$	-1.2557	0.6583	-6.1 <sup>3</sup>
EtOH	$^{13}\text{C}_2$	0.5646	0.5798	-2.6 <sup>3</sup>
EtOH <sup>4</sup>	$^{13}\text{C}_2$	0.2638	0.2402	-2.6 <sup>3</sup>
EtOH <sup>5</sup>	$^{13}\text{C}_2$	1.1469	0.5603	-2.6 <sup>3</sup>
MeOH	$^{13}\text{C}$	1.0408	3.9015	-6.5 <sup>3</sup>
TCM	$^{13}\text{C}$	0.1618	0.2890	1.2 <sup>1</sup>

<sup>1</sup>Ref. 1.

<sup>2</sup>Ref. 2.

<sup>3</sup>Ref. 3 by passive evaporation.

<sup>4</sup>Considering position-specific isotope effects smaller than one.

<sup>5</sup>Considering position-specific isotope effects larger than one.

**Table S2:** VPIEs ( $\varepsilon$  ‰) predicted on evaporation using aug-cc-pvtz basis set for trichlorofluoromethane, dibromomethane, ethanol, methanol, and trichloromethane.

Compound	isotope	$\varepsilon$	STD	Exp.
CFC	$^{12}\text{C}$	0.6429	0.1901	1.7 <sup>1</sup>
DBM	$^{81}\text{Br}$	-0.0206	0.0268	-0.8 <sup>2</sup>
DBM	$^{13}\text{C}$	-0.1737	0.1921	0.6 <sup>2</sup>
EtOH	$^{13}\text{C}_1$	-1.1846	0.6461	-6.1 <sup>3</sup>
EtOH	$^{13}\text{C}_2$	0.4718	0.5618	-2.6 <sup>3</sup>
EtOH <sup>4</sup>	$^{13}\text{C}_2$	0.1734	0.1986	-2.6 <sup>3</sup>
EtOH <sup>5</sup>	$^{13}\text{C}_2$	1.3672	0.2746	-2.6 <sup>3</sup>
MeOH	$^{13}\text{C}$	-0.1250	0.4248	-6.5 <sup>3</sup>
TCM	$^{13}\text{C}$	0.0920	0.2152	1.2 <sup>1</sup>

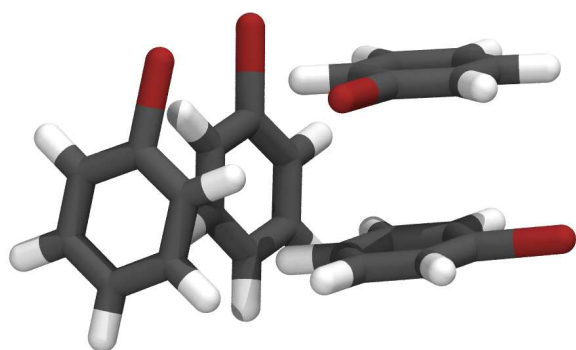
<sup>1</sup>Ref. 1.

<sup>2</sup>Ref. 2.

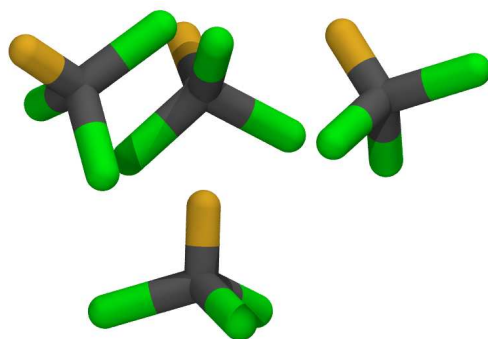
<sup>3</sup>Ref. 3 by passive evaporation.

<sup>4</sup>Considering position-specific isotope effects smaller than one.

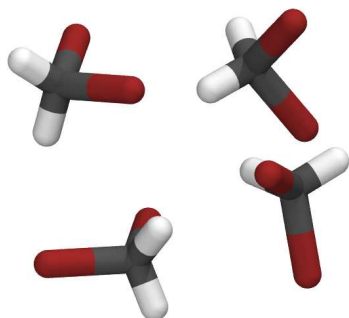
<sup>5</sup>Considering position-specific isotope effects larger than one.



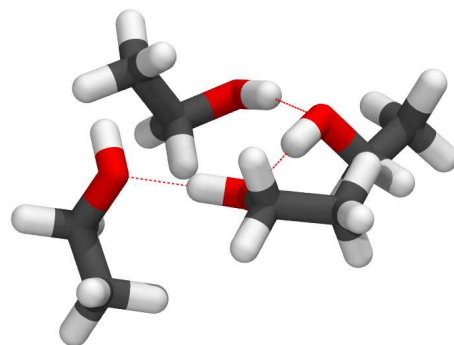
Bromobenzene



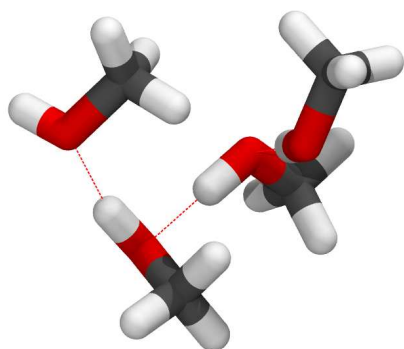
Trichlorofluoromethane



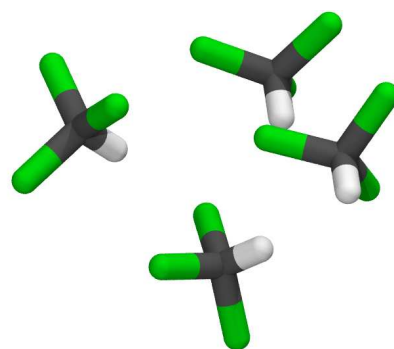
Dibromomethane



Ethanol

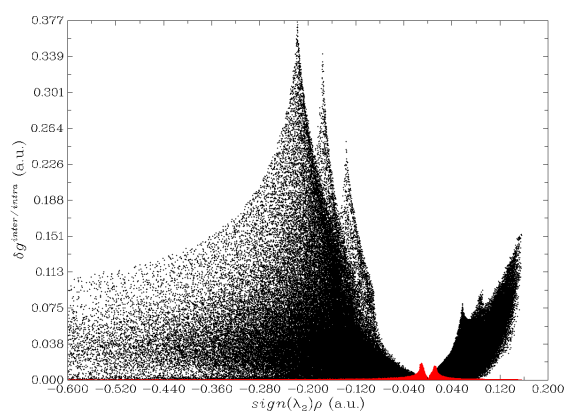


Methanol

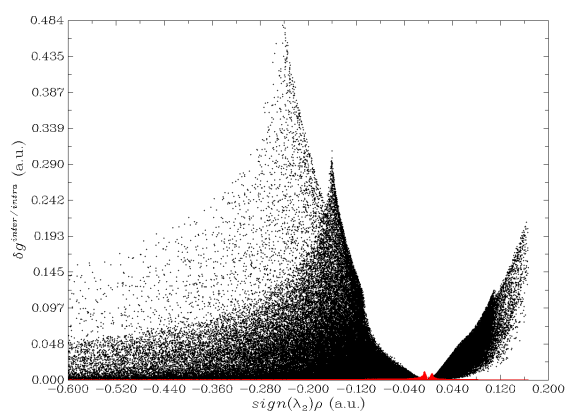


Trichloromethane

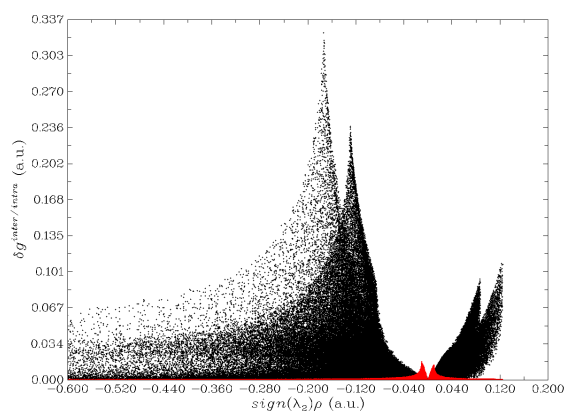
Figure S1: Atomic positions visualisation of compounds cluster used for SAPT and IGM analysis.



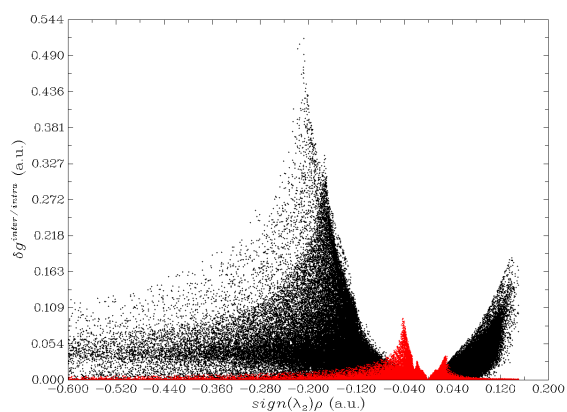
Bromobenzene



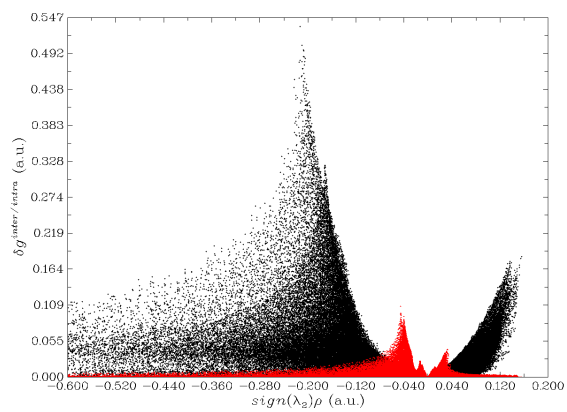
Trichlorofluoromethane



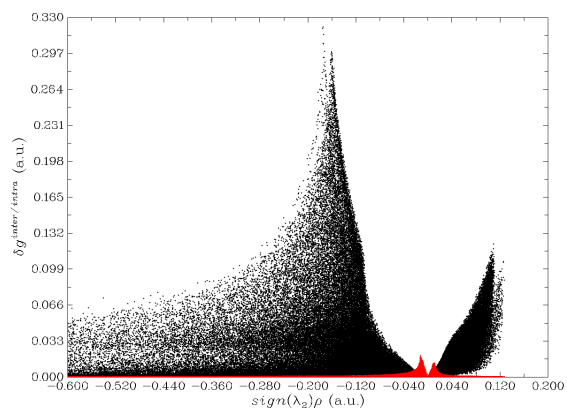
Dibromomethane



Ethanol



Methanol



Trichloromethane

Figure S2: Scattered plot of intermolecular (red) and intramolecular (black) interactions from IGM analysis.

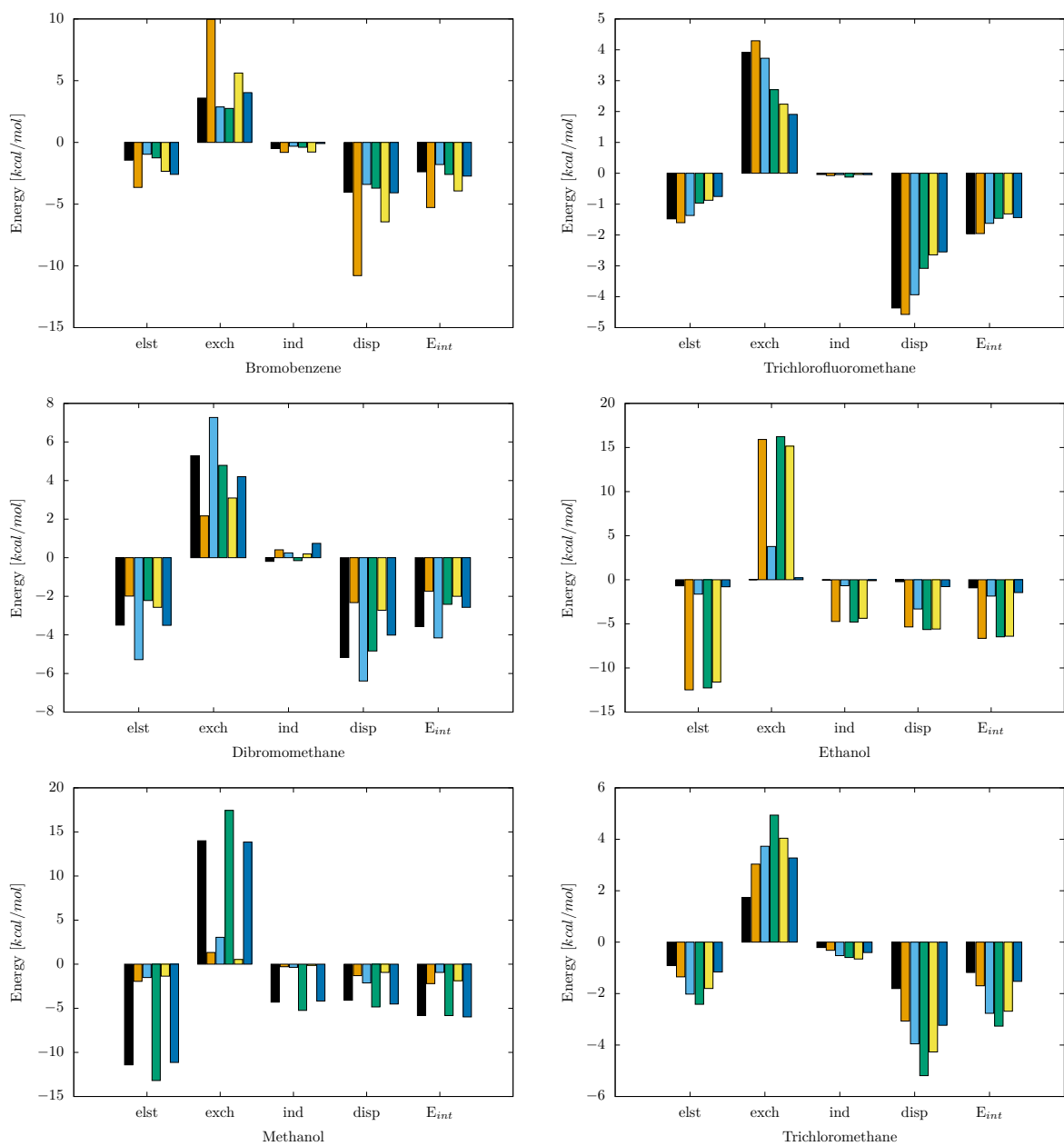


Figure S3: Interaction energy and its decomposition into electrostatics (elst), exchange (exch), induction (ind), and dispersion (disp) for studied compounds of cluster one optimised at  $\omega$ B97x-V/aug-cc-pvdz. Each colour bar indicates one dimer combination, within a four molecule cluster.

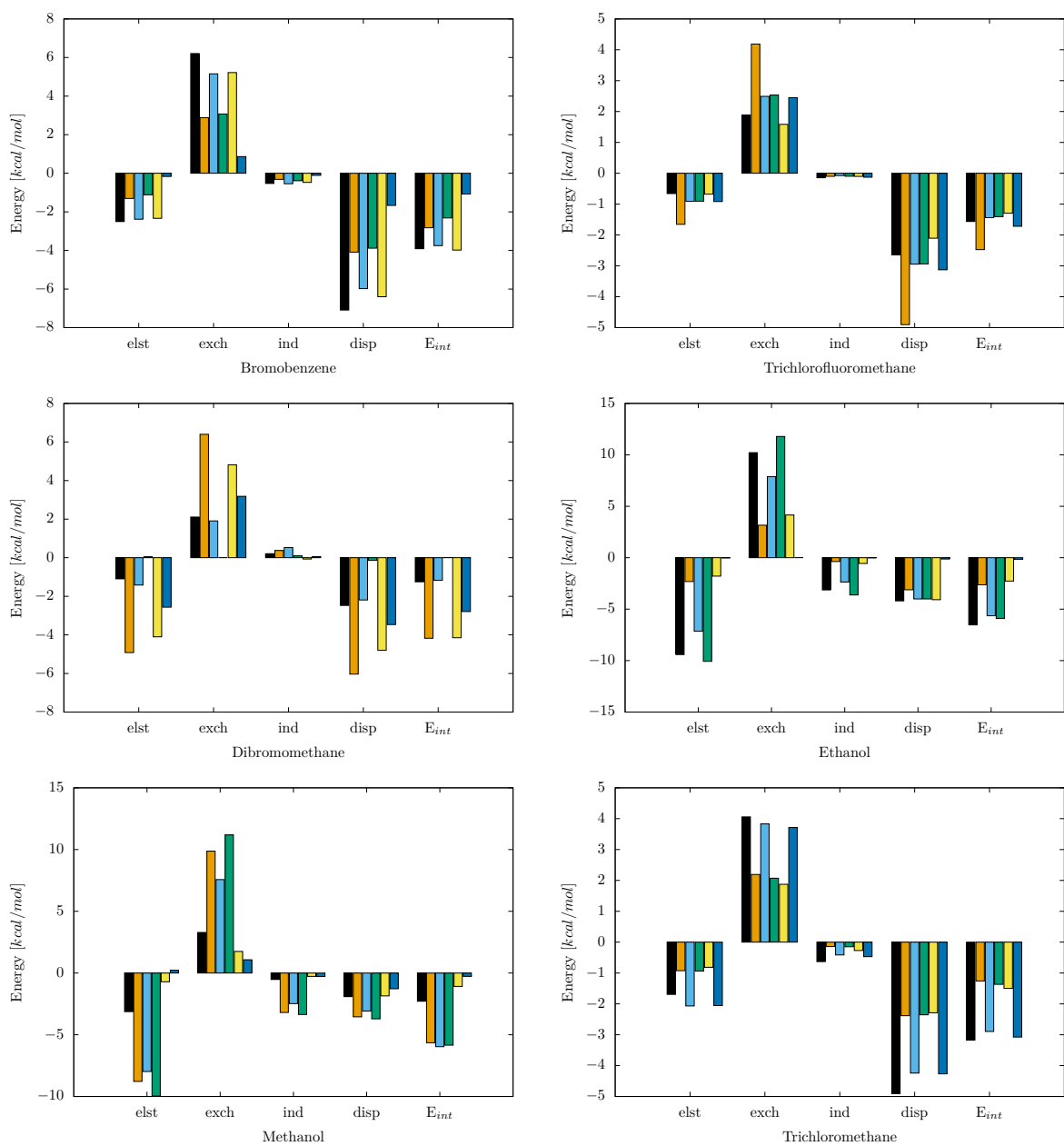


Figure S4: Interaction energy and its decomposition into electrostatics (elst), exchange (exch), induction (ind), and dispersion (disp) for studied compounds of cluster one optimised at  $\omega$ B97x-V/aug-cc-pvdz. Each colour bar indicates one dimer combination, within a four molecule cluster.

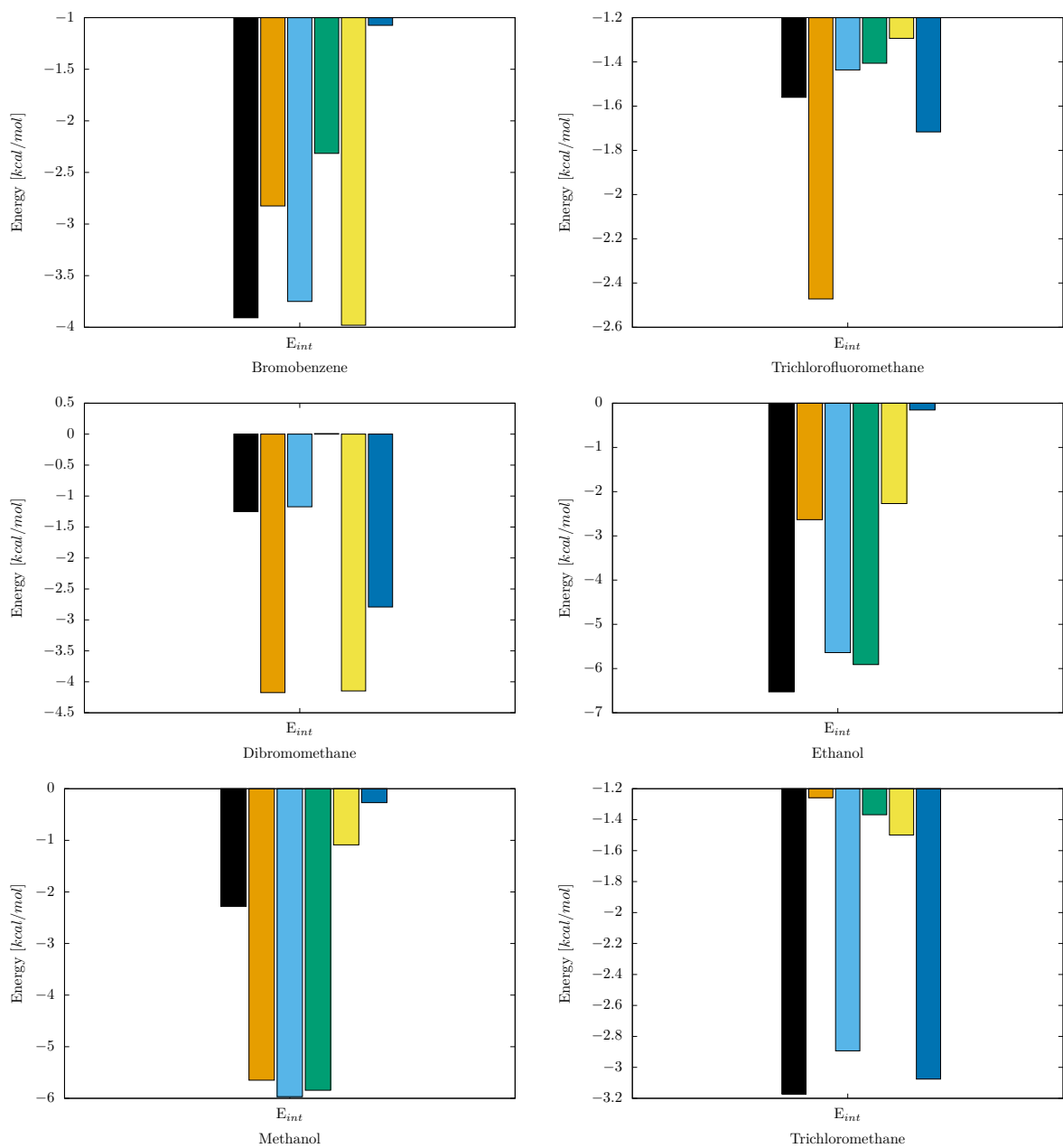


Figure S5: Interaction energy for studied compounds of cluster one optimised at  $\omega$ B97x-V/aug-cc-pvtz. Each colour bar indicates one dimer combination, within a four molecule cluster.

**Table S3:** VPIEs ( $\epsilon$  ‰) predicted on evaporation using aug-cc-pvtz basis set for trichlorofluoromethane, dibromomethane, ethanol, methanol, and trichloromethane.

Compound	isotope	$\epsilon$	STD	Exp.
EtOH	$^{13}\text{C}_1$	-0.9927	0.5353	1.1 <sup>1</sup>
EtOH	$^{13}\text{C}_2$	0.4694	0.4530	0.3 <sup>1</sup>
EtOH <sup>2</sup>	$^{13}\text{C}_2$	0.2355	0.1887	0.4 <sup>1</sup>
EtOH <sup>3</sup>	$^{13}\text{C}_2$	1.1710	0.2403	0.3 <sup>1</sup>
MeOH	$^{13}\text{C}$	0.9342	3.2759	0.5 <sup>1</sup>

<sup>1</sup>Ref. 3 by passive evaporation.

<sup>2</sup>Considering position-specific isotope effects smaller than one.

<sup>3</sup>Considering position-specific isotope effects larger than one.

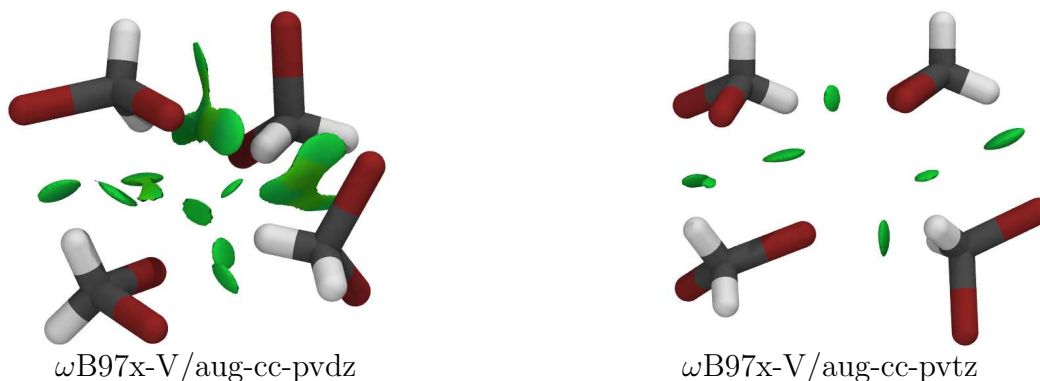


Figure S6: Visualisation of DBM intermolecular interactions by IGM analysis to optimised atomic positions at the  $\omega\text{B97x-V/aug-cc-pvdz}$  (left) and  $\omega\text{B97x-V/aug-cc-pvtz}$  (right) level of theory. BGR colour space describes intermolecular interactions, where blue highlights strong attraction, green are van der Waals interactions, and red are strong repulsive.

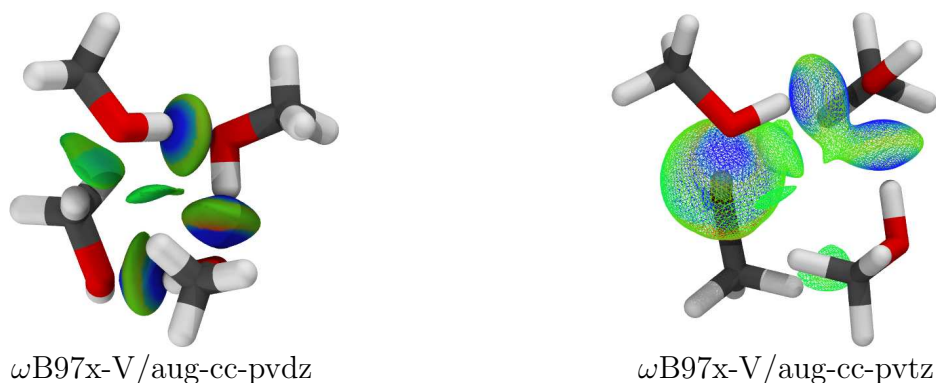


Figure S7: Visualisation of MeOH intermolecular interactions by IGM analysis to optimised atomic positions at the  $\omega\text{B97x-V/aug-cc-pvdz}$  (left) and  $\omega\text{B97x-V/aug-cc-pvtz}$  (right) level of theory. BGR colour space describes intermolecular interactions, where blue highlights strong attraction, green are van der Waals interactions, and red are strong repulsive.

## References

- (1) Horst, A.; Lacrampe-Couloume, G.; Lollar, B. S. Vapor Pressure Isotope Effects in Halogenated Organic Compounds and Alcohols Dissolved in Water. *Analytical Chemistry* **2016**, *88*, 12066–12071.
- (2) Vasquez, L.; Rostkowski, M.; Gelman, F.; Dybala-Defratyka, A. Can Path Integral Molecular Dynamics Make a Good Approximation for Vapor Pressure Isotope Effects Prediction for Organic Solvents? A Comparison to ONIOM QM/MM and QM Cluster Calculation. *The Journal of Physical Chemistry B* **2018**, *122*, 7353–7364.
- (3) Julien, M.; Nun, P.; Robins, R. J.; Remaud, G. S.; Parinet, J.; Höhener, P. Insights into Mechanistic Models for Evaporation of Organic Liquids in the Environment Obtained by Position-Specific Carbon Isotope Analysis. *Environmental Science & Technology* **2015**, *49*, 12782–12788.